A New Generation of Ca²⁺ Indicators with Greatly Improved Fluorescence Properties*

Grzegorz Grynkiewicz‡, Martin Poenie, and Roger Y. Tsien§

From the Department of Physiology-Anatomy, University of California, Berkeley, California 94720

A new family of highly fluorescent indicators has been synthesized for biochemical studies of the physiological role of cytosolic free Ca²⁺. The compounds combine an 8-coordinate tetracarboxylate chelating site with stilbene chromophores. Incorporation of the ethylenic linkage of the stilbene into a heterocyclic ring enhances the quantum efficiency and photochemical stability of the fluorophore. Compared to their widely used predecessor, "quin2," the new dyes offer up to 30-fold brighter fluorescence, major changes in wavelength not just intensity upon Ca²⁺ binding, slightly lower affinities for Ca²⁺, slightly longer wavelengths of excitation, and considerably improved selectivity for Ca²⁺ over other divalent cations. These properties, particularly the wavelength sensitivity to Ca²⁺, should make these dyes the preferred fluorescent indicators for many intracellular applications, especially in single cells, adherent cell layers, or bulk tissues.

Critical evaluation of the role of calcium as an intracellular messenger requires quantitative measurement of cytosolic free Ca²⁺ concentrations, $[Ca^{2+}]_i$,[1] and comparison with varied stimuli and cell responses (1–5). Currently the most popular method for measuring $[Ca^{2+}]_i$ in mammalian cells is to monitor the fluorescence of an indicator called "quin2" (4–7). quin2[2] is loaded into intact cells by incubating them with a membrane-permeant ester derivative. Cytosolic esterases split off the ester groups and leave the membrane-impermeant quin2 tetra-anion trapped in the cytosol. Increases in quin2 fluorescence then signal increased $[Ca^{2+}]$. Although quin2 has revealed much important biological information, it has always

[1] The abbreviations used are: $[Ca^{2+}]_i$, cytosolic free Ca²⁺ concentration; EGTA, ethylene glycol bis(β-aminoethyl ether)-N,N,N′,N′-tetracetic acid; quin2, 2-[[2-[bis(carboxymethyl)amino]-5-methylphenoxy]methyl]-6-methoxy-8-[bis(carboxymethyl)amino]quinoline; BAPTA, 1,2-bis-(2-aminophenoxy)ethane-N,N,N′,N′-tetraacetic acid; MOPS, 3-(N-morpholino)propanesulfonic acid; DMF, dimethylformamide; dansyl, 5-dimethylaminonaphthalene-1-sulfonyl.

[2] Quin2 was originally written (7) with no hyphen, so that word processors would not separate the letters from the numeral. This simple name has subsequently been misquoted with nearly all conceivable variations of punctuation, capitalization, and even Roman numerals. Unfortunately fura-1, indo-1, and most of all stil-1 must have punctuation to distinguish the numeral 1 from the letter l, so that all the new dyes are named with hyphens.

had severe and acknowledged limitations (5, 7). Its preferred excitation wavelength of 339 nm is too short, since such UV irradiation excites significant autofluorescence from cells, could cause biological side effects, and penetrates microscope optics poorly. 2) Its extinction coefficient (<5000) and fluorescence quantum yield (0.03 to 0.14), although comparable to dansyl groups in aqueous solution, are too low. These spectroscopic properties mean that quin2 loadings of several tenths of millimolar or more are necessary to overcome cell autofluorescence. In some cell types, this much loading significantly buffers $[Ca^{2+}]_i$ transients. 3) Quin2 signals Ca²⁺ by increasing its fluorescence intensity without much shift in either excitation or emission wavelengths. Unfortunately, fluorescence intensity is also dependent on many other poorly quantified or variable factors such as illumination intensity, emission collection efficiency, dye concentration, and effective cell thickness in the optical beam. It would be much better to have an indicator that responded to calcium by shifting wavelengths while maintaining strong fluorescence. The ratio of the fluorescences at two suitably chosen wavelengths would then signal calcium while cancelling out most or all of the possible variability due to instrument efficiency and content of effective dye. 4) The high effective affinity of quin2 for Ca²⁺ is ideal for measuring levels near or below typical resting values of $[Ca^{2+}]_i$ near 10^{-7} M, but also means that at micromolar levels or above, the dye approaches saturation and loses resolution. Dyes with weaker affinities are needed to quantify such elevated levels. 5) Finally, the selectivity of quin2 for calcium over magnesium and heavy metal divalent cations could bear improvement. Quin2 binds Mg²⁺ with a dissociation constant of 1–2 mM. Although Mg²⁺ has little effect on the fluorescence of quin2 when excited at 339 nm, variations in $[Mg^{2+}]_i$ would affect the effective affinity for Ca²⁺ and the calibration scale for the fluorescence signals. Also, cells with unusually high levels of exchangeable heavy metals can give falsely low readings of $[Ca^{2+}]_i$ because the heavy metals quench quin2 fluorescence (8). Conversely, dye loading could perturb $[Mg^{2+}]_i$ or chelate heavy metals important in cell functions. Greater selectivity for binding Ca²⁺ instead of Mg²⁺ or heavy metal ions is observed in related tetracarboxylate chelators in which the rings are linked by ether linkages without any quinoline ring nitrogen (6).

This report describes the synthesis and chemical properties of a new group of six Ca²⁺ indicators. Compared to quin2, they show much stronger fluorescence, wavelength shifts upon Ca²⁺ binding, somewhat weaker affinity for Ca²⁺, and better selectivity against magnesium and heavy metals. The six new chelators described combine a stilbene fluorophore with the octacoordinate, tetracarboxylate pattern of liganding groups (6) characteristic of EGTA and BAPTA. The most promising members, fura-2 and indo-1, contain extra heterocyclic bridges to reinforce the ethylenic bond of the stilbene and to

reduce hydrophobicity. The new indicators should not only supersede quin2 in many applications, but also ease $[Ca^{2+}]_i$ measurements in adherent cells, bulk tissues, or single cells under a microscope or in a flow cytometer.

Biological applications of the new indicators are reported in separate papers.

EXPERIMENTAL PROCEDURES[3]

The synthetic routes to the new indicators are outlined in Figs. 1 and 2. Full descriptions of the reaction conditions are described in the Miniprint Supplement.

UV absorbance spectra were recorded on a Cary 210 spectrophotometer at 22 ± 2 °C. Fluorescence spectra were recorded either on a Perkin-Elmer MPF-44A spectrofluorometer or on a Spex Fluorolog 111, both in ratio mode with rhodamine B quantum counters. Correction factors for the emission monochromator and photomultiplier were obtained by comparing the spectra of reference compounds with their known quantum distributions (9). The quantum yields were determined by comparing the integral of the corrected emission spectrum of the test sample with that of a solution of quinine bisulfate in 1 N sulfuric acid. The concentration of quinine was adjusted to give the same absorbance as the sample at the exciting wavelength. The quantum efficiency of quinine was taken to be 0.55 (10).

Free $[Ca^{2+}]$ levels were controlled by Ca^{2+}/EGTA buffers assuming apparent dissociation constants for the $Ca^{2+} \cdot$ EGTA complex of 380 nM at pH 7.00 in 100 mM KCl, 20 °C; 151 nM at pH 7.20 in 100 mM KCl, 20 °C; 214 nM at pH 7.05 in 130 mM KCl, 20 mM NaCl at 37 °C; and 490 nM at pH 7.02 in 225 mM KCl, 25 mM NaCl at 18 °C. The first three apparent dissociation constants were calculated from the tables of Martell and Smith (11) as discussed in Refs. 1 and 12. The last value was freshly determined in this study because no appropriate absolute constants were available at the higher ionic strength, and existing estimates in the biological literature (13–17) vary by an unacceptably large range, >0.5 log unit. For this determination we chose the classic and reliable method of pH titration in the presence and absence of excess metal ion (18). Details are included in the Miniprint Supplement.

Free $[Mg^{2+}]$ was likewise controlled by Mg^{2+}/EGTA buffers assuming an apparent dissociation constant for the $Mg^{2+} \cdot$ EGTA complex (including its monoprotonated form) of 21 mM at pH 7.18 in 130 mM KCl at 20 °C, 8.96 mM at pH 7.05 in 130 mM KCl, 20 mM NaCl at 37 °C, and 99 mM at pH 7.02 in 255 mM KCl, 25 mM NaCl at 18 °C. Again, the last value was freshly determined in this study. Heavy metal binding constants were measured as described in the Miniprint Supplement.

Binding to membranes was assessed by adding 0.3-ml portions of well-washed, packed human red cells to 1.5 ml volumes of 2 μM fura-2, fura-3, or indo-1, in media containing 145 mM NaCl, 5 mM KCl, 10 mM Na/MOPS at pH 7.4, 1 mM Na_2HPO_4, 1 mM $MgCl_2$, and either 1 mM EGTA or 1 mM $CaCl_2$. After several minutes of equilibration, the red cells were removed by centrifugation, and the fluorescence of the supernatant was measured with front-face geometry. An upper limit on the binding of dye to the membranes was estimated from the slight loss of fluorescence in the supernatant compared to the fluorescence before any cells had been added. This difference gives only an upper limit because dilution by residual extracellular water in the packed red cells or inner filter effects of hemoglobin released from a few damaged cells would also have tended to depress the fluorescence.

RESULTS

Organic Syntheses—The key intermediate in the synthesis of stil-1, stil-2, and indo-1 is the aldehyde VII. The methyl group on the right-hand benzene ring is useful because it blocks electrophilic substitution there, restricting formylation

to the left-hand ring. The methyl group is also expected (6) to increase slightly the cation affinities of the final chelators. Aldehyde VII and various benzylic phosphoranes (VIII, XI, and XIV) are linked by Wittig reactions to build the extended conjugation chain. The indole ring in indo-1 is constructed by using triethyl phosphite to reduce the nitro group of XV and generate a nitrene which immediately cyclizes (19).

Fura-1, fura-2, and fura-3 all arise from the salicylaldehyde derivative XXV, itself synthesized in eight steps from *p*-hydroquinone. Key steps in the preparation of the salicylaldehyde include the acid-catalyzed, selective debenzylation (20) of the phenolic group *ortho* to the nitro in preference to the phenolic group *meta* to nitro. Attempts to convert XXIV to XXV by hydroxide displacement of benzyloxide were unsuccessful. The remaining benzyl protecting group survives hydrogenation with platinum catalysis (21) and Vilsmeier formylation but is finally removed by hydrogenation with palladium. The phenolic hydroxyl is remade into an ether with an electronegatively substituted benzyl group. A base-catalyzed Knoevenagel reaction then completes the benzofuran ring. Potassium fluoride on alumina is a particularly good catalyst for this condensation (22) perhaps because it has less tendency than other bases to attack the ester groups also present.

The procedure for preparing the acetoxymethyl esters of the chelators was changed from the previous method (23), which had been to prepare the dry, solid free acid form of the chelator and react it with acetoxymethyl bromide in the presence of a hindered base, ethyldiisopropylamine. This procedure had given acceptable results with simpler BAPTA series chelators but proved erratic in yield and purity when applied to more complex derivatives such as the new dyes described here. One problem was found to be the purity of the acetoxymethyl bromide, heretofore prepared from acetyl bromide and paraformaldehyde and contaminated with a few mole per cent of bis(bromomethyl)ether as a nearly inseparable by-product (24). This ether seems to react faster than the carboxylic acid than the acetoxymethyl bromide does, yielding esters poorly hydrolyzable by cells. The percentage of such esters of course increases if a large excess of the crude bromide is used, and decreases if the bromide is partially purified by vacuum distillation through a spinning-band column. However, the best solution is to prepare acetoxymethyl bromide by an alternate route that generates no bis(bromomethyl)ether. Such a route was eventually found in the cleavage of methylene diacetate with trimethylsilyl bromide, a reaction that seems to stop cleanly with the formation of acetoxymethyl bromide, not methylene dibromide. Another change of procedure was to avoid isolation of the chelators as dry solid free acids, a process that seemed to cause partial decomposition, perhaps by decarboxylation. Instead the chelator esters were saponified with tetrabutylammonium hydroxide to give tetrabutylammonium salts that were sufficiently soluble in polar organic solvents to be reacted with acetoxymethyl bromide.

Absorbance Spectra—Absorbance and fluorescence properties for the new indicators in the presence and absence of Ca^{2+} are compiled in Table I. The absorbance spectra are much as one would expect for stilbene chromophores. Absorbance maxima are in the near UV, with extinction coefficients in the range 2–3 $\times$ 10^4 M^{-1} cm^{-1}. The binding of Ca^{2+} shifts all the absorbance spectra to shorter wavelengths.

Fluorescence Properties—In all these indicators, both the calcium-free and calcium-bound species fluoresce quite strongly, a feature that was a prime motivation for developing

---

[3] Portions of "Experimental Procedures" are presented in miniprint at the end of this paper. Miniprint is easily read with the aid of a standard magnifying glass. Full size photocopies are available from the Journal of Biological Chemistry, 9650 Rockville Pike, Bethesda, MD 20814. Request Document No. 84M-2660, cite the authors, and include a check or money order for $4.40 per set of photocopies. Full size photocopies are also included in the microfilm edition of the Journal that is available from Waverly Press.
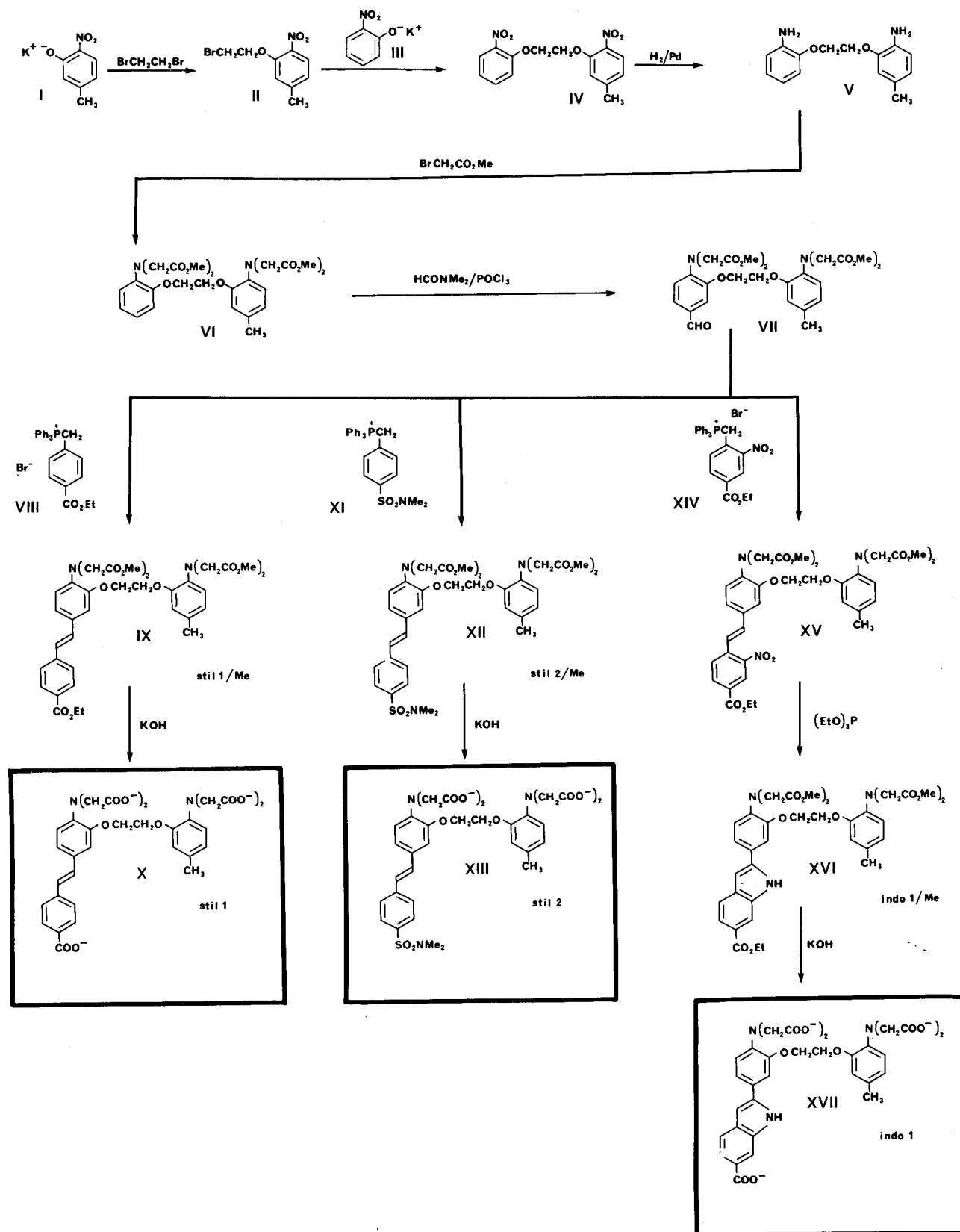
FIG. 1. **Synthetic pathway leading to stil-1, stil-2, and indo-1.** Roman numerals are keyed to the synthetic details in the Miniprint Supplement.
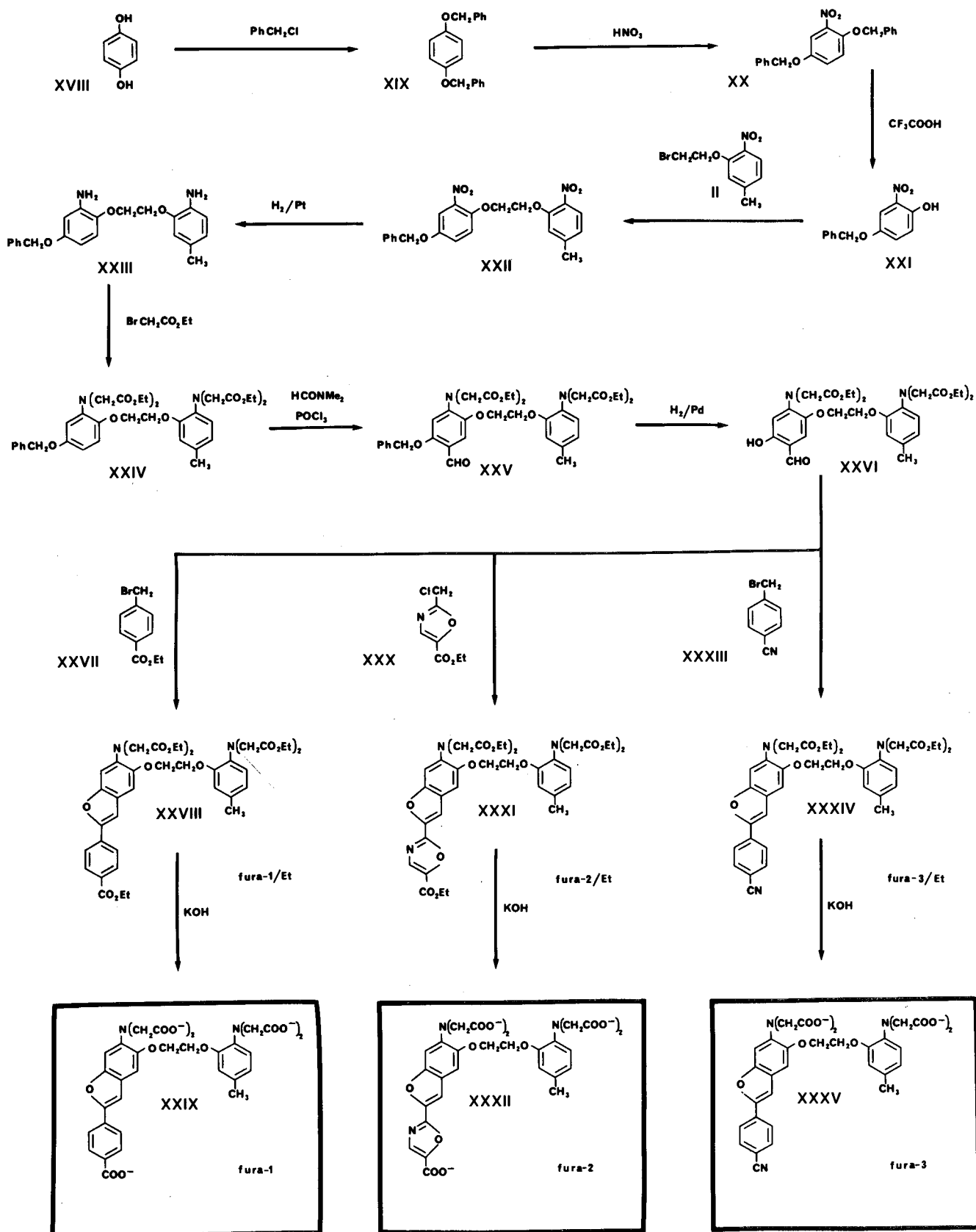
FIG. 2. Synthetic pathway leading to fura-1, fura-2, and fura-3.

New Fluorescent Ca²⁺ Indicators

TABLE I

Properties of new fluorescent indicators of Ca²⁺

Absorption maxima refer to the dominant peaks at longest wavelength, measured at 22 ± 2 °C in 100 mM KCl. The first number is the wavelength in nanometers, followed in parentheses by $10^{-3} \times$ the corresponding extinction coefficient, M^{-1} cm^{-1}. The data for stil-2 are for the *cis-trans* mixture as saponified; both the wavelengths and extinction coefficients would increase for pure *trans*. Extinction coefficients for fura-1 and fura-3 may be underestimated since less effort was expended on their purification than on stil-1, indo-1, and fura-2. Emission maxima list the peak wavelengths in nanometers of the uncorrected and corrected (in parentheses) emission spectra. The differences between uncorrected and corrected values are greatest for stil-1 and fura-1 because they were measured on the Perkin-Elmer MPF44, whose emission characteristics are more biased than the Spex Fluorolog, on which the others were determined. Emission maxima and quantum efficiencies were measured in 100 mM KCl, 22 ± 2 °C.

Dye	Apparent K_d for Ca²⁺	Absorption maxima		Emission maxima		Fluorescence quantum efficiency	
		Free anion	Ca complex	Free anion	Ca complex	Free anion	Ca complex
	nM						
stil-1	132[a], 200[b]	362 (27)	329 (34)	537 (585)	529 (ND[c])	0.14	ND
stil-2	224[d]	352 (12)	326 (12)	564 (590)	560 (587)	0.11	0.15
indo-1	250[b]	349 (34)	331 (34)	485 (482)	410 (398)	0.38	0.56
fura-1	107[b]	350 (21)	334 (27)	534 (585)	522 (548)	0.14	0.20
fura-2	135[a], 224[b]	362 (27)	335 (33)	512 (518)	505 (510)	0.23	0.49
fura-3	140[b]	370 (14)	343 (25)	564 (588)	551 (599)	0.13	0.21

[a] In 100 mM KCl, 20 °C, pH 7.1–7.2.
[b] In 115 mM KCl, 20 mM NaCl, 10 mM-K-MOPS, pH 7.05, 1 mM free Mg²⁺, 37 °C.
[c] ND, not determined.
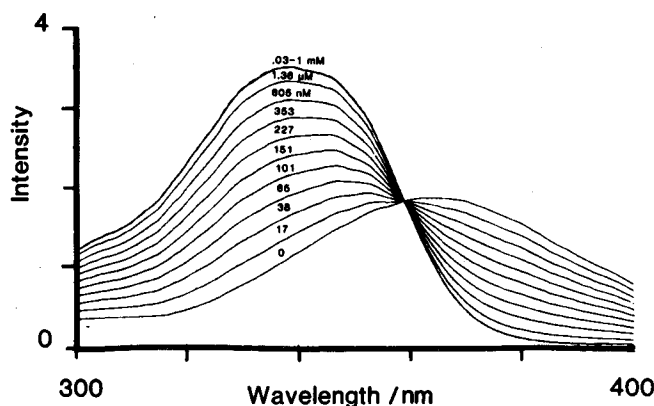[d] In 100 mM KCl, 37 °C, pH 7.08.

FIG. 3. **Excitation spectra for 1 μM fura-2 at 20 °C in buffers with free Ca²⁺ values ranging from <1 nM to >10 μM.** The excitation band width was 1.9 nm, the emission was collected at 510 nm with 4.6 nm band width, and the spectra were automatically corrected for excitation lamp and monochromator characteristics using a rhodamine B quantum counter. The titration was done starting with 5 ml of 100 mM KCl, 10 mM K-MOPS, 10 mM K₂H₂EGTA, 1 μM fura-2, adjusting the pH to 7.20, recording the spectrum, then discarding 0.5 ml of this solution and replacing with 0.5 ml of 100 mM KCl, 10 mM K-MOPS, 10 mM K₂CaEGTA, 1 μM fura-2, readjusting the pH to 7.20, and recording the spectrum which was then in 9 mM K₂H₂EGTA and 1 mM K₂CaEGTA. Subsequent iterations to reach n mM CaEGTA, (10-n) mM EGTA, n = 2–10, were done by discarding 5.0/(11-n) ml and replacing with equal volumes of the 10 mM K₂CaEGTA, 1 μM fura-2 stock. After n = 10 had been reached to give a free Ca²⁺ between 10⁻⁴ and 10⁻⁵ M, addition of 1 mM CaCl₂ had no further effect on the spectrum. Equality of Ca and EGTA contents in the K₂CaEGTA solutions was insured by titration of K₂H₂EGTA and CaCl₂ to the potentiometric end point measured with a Ca²⁺ selective electrode. EGTA was Fluka Chemical "puriss." grade.

this series. The fluorescence excitation spectra shift to shorter wavelengths as [Ca²⁺] increases, much as the absorption spectra do. An example is shown in Fig. 3, a set of excitation spectra for fura-2 in calibration buffers of varied [Ca²⁺]. Given such calibration data, the [Ca²⁺] in an unknown solution

containing the dye can be deduced from the shape of the excitation spectrum. An explicit formula for this calibration is derived under "Discussion." For all the dyes except indo-1, the binding of Ca²⁺ shifts the wavelengths of the emission maxima much less than it shifts the excitation maxima. The exception, indo-1, emits near 400 nm in its Ca²⁺ complex compared to about 480 nm when free. Indo-1 emission spectra show a clear crossover point whose position depends on the excitation wavelength because that affects the relative efficiency with which Ca²⁺-free and Ca²⁺-bound forms are excited. At an excitation wavelength of 355–356 nm as would be produced by a krypton laser, indo-1 gives the family of emission spectra shown in Fig. 4 in which the long and short wavelength peaks are of comparable amplitude.

The quantum yields of fluorescence for the new indicators range up to ~0.5 for indo-1 and fura-2 with Ca²⁺. Such values are typical of dyes normally considered to be highly fluorescent. In all cases the Ca²⁺ complex has a quantum efficiency between 1.3- and 2.1-fold higher than the Ca²⁺-free dye. For comparison, the quantum efficiencies of quin2 with and without Ca²⁺ are 0.14 and 0.029, respectively (6). Since fura-2 at half-saturation has a quantum efficiency four to five times higher than quin2 at half-saturation, and fura-2 has extinction coefficients about six times higher than quin2, the fluorescence intensity/molecule of fura-2 should be about 30 times greater than that for quin2. Indeed Fig. 5 shows that the fluorescence intensities of 1 μM fura-2 and of its Ca²⁺ complex are comparable to 30 μM quin2 and its complex examined under similar conditions.

Ca²⁺-binding Constants—Dissociation constants for all the new chelators (Table I) are in the range 100–300 nM at ionic strengths near 0.1–0.15. Such values are close to the dissociation constant (110 nM) of the parent compound BAPTA (6). The substituents that make up the rest of the chromophores must be only slightly electron-withdrawing, because moderately electron-withdrawing substituents such as halo, azo, and acyl cause much larger increases in Ca²⁺-dissociation constants (4). Fura-2 was also examined at higher ionic strengths, ~250 mM (225 mM KCl, 25 mM NaCl). A considerable de-
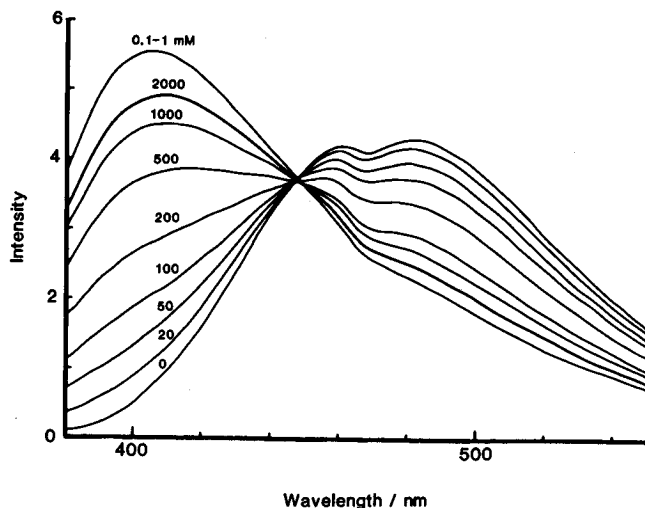
FIG. 4. **Emission spectra for indo-1 as a function of free Ca²⁺.** The dye, 6 μM, was titrated in 115 mM KCl, 20 mM NaCl, 10 mM MOPS, 1.115 mM MgCl₂, 1.115 mM K₂H₂EGTA, KOH to pH 7.050 ± 0.004, 37 °C, to which small aliquots of K₂CaEGTA were added from a micrometer syringe to raise free Ca²⁺ to the values labeling each curve, in units of nanomolar unless otherwise specified. Excitation was at 355 nm, and both excitation and emission were set to 5 nm band width. These spectra are not corrected for the emission sensitivity characteristics of the Perkin-Elmer MPF-44; in particular the notch at 465 nm is an instrumental artifact. Corrected emission spectra show the low-Ca 485 nm peak to be of very similar amplitude to the high-Ca 404 nm peak when excitation is at 355–356 nm.

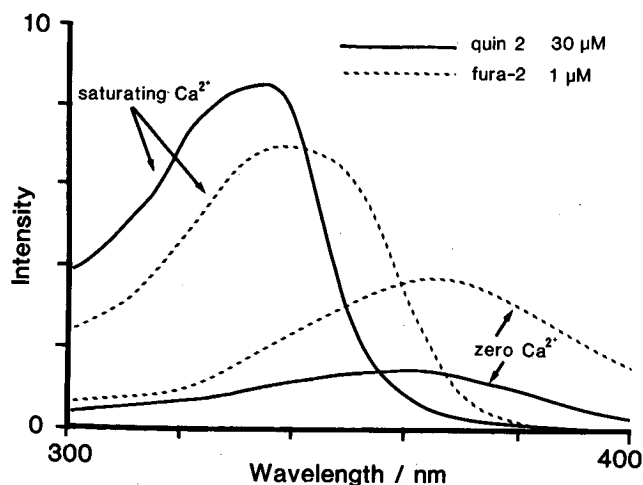FIG. 5. **Excitation spectra of 1 μM fura-2 and 30 μM quin-2 under identical sets of conditions: 130 mM KCl, 10 mM MOPS, 1 mM EDTA, KOH to pH 7.20, 20 °C, before and after addition of 2 mM CaCl₂ to give 1 mM free Ca²⁺.** Emission was collected at 500 nm, 4.6 nm band width, and the excitation band width was 0.93 nm. Quin2-free acid was from Lancaster Synthesis, Morecambe, England.

crease in Ca²⁺ binding strength was observed, to an apparent dissociation constant of 760 nM. Such a strong dependence on ionic strength is not surprising for the reaction of a tetravalent anion with a divalent cation.

Photoisomerization of Stilbenes—Preliminary studies (not shown) indicated that the photochemistry of stil-1 and stil-2 is complicated enough to limit their utility as Ca²⁺ indicators. These two dyes can exist in *cis* and *trans* isomers because they lack the extra rings built into the later dyes. Both isomers are included in the products (IX, XIII, and IX) of the Wittig reactions. Separation of the isomers was attempted only with stil-1/Me and Et. Thin layer chromatography (chloroform/

methanol, 9:1 or 19:1, v/v) on AgNO₃-impregnated silica was barely able to resolve the two isomers of stil-1/Et, the *cis* isomer migrating more slowly. High pressure liquid chromatography on an octadecyl reverse phase column (Supelcosil LC-18 25 cm × 4.6 mm, Supelco, Inc., Bellefonte, PA) and methanol/water (92:8, v/v) elution also separated the isomers. In each case the *cis* isomer was identified by its nonfluorescence. Preparative isolation of the desired *trans* isomer was best accomplished by repeated recrystallization of the ester, stil-1/Me. Saponification of the pure *trans* ester in the dark was assumed to give pure *trans* penta-anion. Irradiation of the anion in aqueous solution with 365 nm light reduced both the long wavelength absorbance and the fluorescence. Assuming only the *trans* isomer is fluorescent (25), the photostationary state in the absence of Ca²⁺ contains about 75% *trans*, 25% *cis*. This ratio of *trans* to *cis* is unusually high for a stilbene photostationary state. Photoisomerization significantly complicates the use of *trans* stil-1 as a fluorescent indicator. It becomes necessary to irradiate stil-1 strongly to reach photostationary equilibrium before Ca²⁺ measurement begins. Those measurements must then be made with minimum intensity of the excitation beam. The [Ca²⁺] should be deduced from the ratio of excitation efficiencies at two wavelengths rather than from the absolute fluorescence intensity at any one excitation wavelength. Unfortunately, stil-1 also undergoes yet another, albeit slow, photochemical reaction in addition to *cis-trans* isomerism. This slow reaction causes a gradual rise in fluorescence at long (>380 nm) excitation wavelengths. It is most noticeable when a stil-1 sample is irradiated at very low [Ca²⁺], then exposed to high Ca²⁺ during measurement of its excitation spectrum. A plausible but unproven explanation is the photocyclization of the non-fluorescent *cis* isomer to a phenanthrene (25) which could be quite fluorescent at the longer excitation wavelengths. All these complications of stilbenes were prime motivations for the design and synthesis of the indo and fura dyes, in which such photochemical reactions are prevented by heterocyclic ring formation.

Cation Selectivity—Binding constants for competing cations were most thoroughly explored for fura-2. Titrations with Mg²⁺ (Fig. 6) showed dissociation constants of about 5.6 mM at 37 °C and 9.8 mM at 20 °C at 0.1–0.15 M ionic strength. Therefore fura-2 binds Mg²⁺ less strongly than does quin2, whose Mg²⁺ dissociation constants are about 1 and 2 mM, respectively, at 37 and ~22 °C (6, 7). Furthermore, the effect of Mg²⁺ binding on the fura-2 spectrum is quite small compared with the effect of Ca²⁺, as may be seen by comparing Fig. 6 with Fig. 3. At extremely high Mg²⁺ levels (100 mM or greater), the excitation spectra decrease in peak amplitude and no longer pass through the crossover point near 377 nm that is common to all the curves in Fig. 6. This behavior may reflect partial formation of 2:1 (Mg²⁺/dye) complexes and was not further explored.

Binding of fura-2 to some of the physiologically more important heavy divalent metal ions was also briefly examined. Both stil-1 and fura-2 bind zinc with dissociation constants around 1.6–2 nM (pKZn 8.6–8.8). Although these values are about 100 times lower than those for the Ca²⁺ complexes, the selectivity of stil-1 and fura-2 for Ca²⁺ is considerably better than that of quin2, whose Zn²⁺ complex has a Kd about 1/3000 that of its Ca²⁺ complex (26). Curiously, Zn²⁺ shifts the fura-2 spectrum the same way that Ca²⁺ does, whereas Zn²⁺ quenches quin2 and therefore acts oppositely to Ca²⁺. Fura-2 is also better than quin2 in rejecting Mn²⁺, the Mn²⁺/Ca²⁺ preferences being 42-fold and 510-fold, respectively (26). The predominant oxidation state of labile intracellular iron
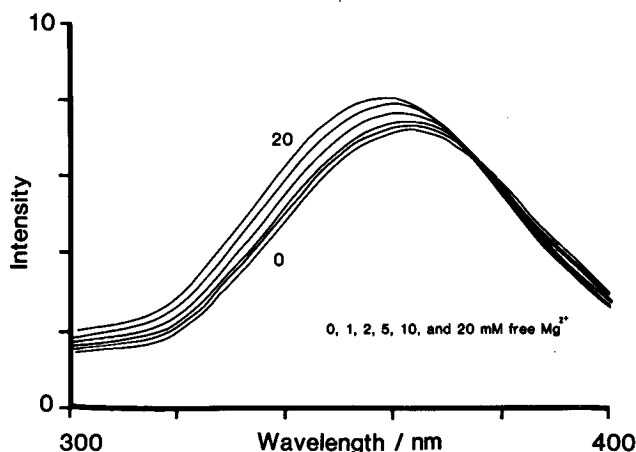
FIG. 6. **Effect of Mg^{2+} on fura-2.** An excitation spectrum was recorded of 2 μM fura-2 in 2.5 ml of 132 mM KCl, 1 mM EGTA, 10 mM MOPS, adjusted with KOH to pH 7.18 while thermostatted at 20 °C. Then 25 μl of this solution was discarded and replaced by 25 μl of a solution containing 2 μM fura-2, 104.8 mM MgCl$_2$, 5.8 mM EGTA, 10 mM MOPS, adjusted with KOH to pH 7.18. Since both stocks had 1 mM free EGTA but the latter had 100 mM free Mg, the 99:1 (v/v) composite went to 1.0 mM free Mg^{2+}. Further iterations attained 2, 5, 10, and 20 mM free Mg^{2+} by successively discarding 25.25, 76.53, 131.6, and 277.8 μl of the mixture and replacing each with an equal volume of the high-Mg stock. Emission was collected at 510 nm, 4.6 nm band pass, and excitation 0.9 nm band pass.
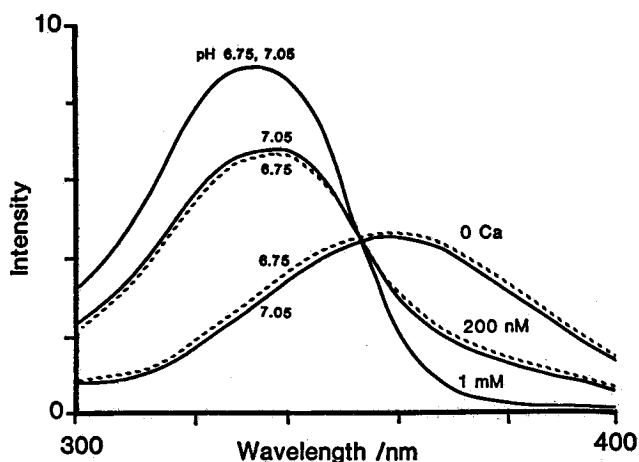

FIG. 7. **Effect of pH excursion between 6.75 and 7.05 on fura-2 at 0, 200 nM, and 1 mM free Ca^{2+}.** An excitation spectrum of 0.5 μM fura-2 was recorded in 135 mM KCl, 5 mM MOPS, 2 mM EGTA, adjusted with KOH to pH 7.05 at 37 °C. The succeeding spectra were taken following acidification with HCl to pH 6.75; addition of 0.379 mM CaCl$_2$ and KOH to pH 6.75; addition of 0.655 mM more CaCl$_2$ and KOH to pH 7.05; addition of 2 mM CaCl$_2$ and KOH to pH 6.75; KOH to pH 7.05. A record was kept of the volumes added, so that the spectra shown have been scaled to compensate for the slight dilution effects. Emission was collected at 505 nm, 18.5 nm band pass, with 4.6 nm excitation band pass. The curves with 200 nM free Ca were important to include because there might have been an important protonation, perhaps on the amino nitrogen of the right-hand ring, that would significantly inhibit Ca^{2+} binding without affecting the fluorescence in either 0 Ca^{2+} or overwhelmingly high Ca^{2+}. The observation that at 200 nM Ca^{2+} the pH 6.75 curve is closer than the pH 7.05 to the "0 Ca" curve suggests that such an H^{+} inhibition of Ca^{2+} binding does take place to a small extent, but the effect is clearly small and is partly neutralized by the slight direct effect of pH on the Ca^{2+}-free dye.

is +2 (27); Fe^{2+} binds fura-2 between 3 and 10 times as strongly as Ca^{2+} does. A more precise estimate was prevented by experimental scatter, which may reflect more complicated

stoichiometry than 1:1 or imperfectly anaerobic conditions. Both Mn^{2+} and Fe^{2+} quench fura-2 as expected for metal ions with many unpaired electrons. For comparison, EGTA prefers Zn^{2+}, Mn^{2+}, and Fe^{2+} to Ca^{2+}, by factors of ~50, ~20, and ~8-fold, respectively (11).

The effects on fura-2 of pH changes within the physiological range seem to be very small. Fig. 7 indicates that pH variations over a reasonable range of intracellular values hardly affect either the spectra of the Ca^{2+}-free or Ca^{2+}-bound species or the effective Ca^{2+} dissociation constant.

Binding to Membranes—Red cells were used as model membranes easy to add and remove. Red cells added to a hematocrit of 17% in a solution of fura-2, fura-3, or indo-1, then centrifuged out, decreased the fluorescence of the supernatant by less than 5%. This small drop in fluorescence could have been just dilution by the small unavoidable amount of extracellular fluid added with the packed cells. Even if it were attributed entirely to binding, the amount of dye bound to a membrane would be less than that contained in a layer 0.2 μm thick of adjacent aqueous solution. Such negligible binding was found whether the medium contained 1 mM Ca^{2+} or EGTA without Ca^{2+}.

DISCUSSION

Increased brightness of fluorescence is the most dramatically noticeable advantage of these new dyes over their immediate predecessors such as quin2. The increase of about 30-fold in fluorescence can be used to decrease intracellular dye loadings and buffering of cytosolic [Ca^{2+}] transients. Alternatively the brightness can permit Ca^{2+} measurement in shorter observation times or from smaller volumes of tissue. An example of the latter is the observation[4] with fura-2 of rises in [Ca^{2+}]$_i$ induced by mitogenic lectins in solitary thymocytes of about 6 μm diameter, an experiment that was not successful when tried with quin2 (28).

Another major feature of the new dyes is the ability of Ca^{2+} to alter the wavelengths not just amplitudes of the fluorescence excitation or emission peaks. Although quin2 also shifts its peak excitation wavelength upon binding Ca^{2+} (Fig. 5), this shift is hard to use because the long-wavelength end of its excitation spectrum has too low an intensity and is too sensitive to Mg^{2+}. Therefore quin2 has almost always been used with excitation centered on 339 nm. Under these conditions any given fluorescence reading from intracellular quin2 has no quantitative meaning until compared with an end of experiment destructive calibration in which the dye is forced into two known states of high and low Ca^{2+} saturation. Any intervening loss of dye or change in instrument sensitivity jeopardizes the calibration and may be mistaken for a change in [Ca^{2+}]$_i$. By contrast, if a dye shifts wavelengths upon binding Ca^{2+}, the ratio R of the dye's fluorescence intensities F_1 and F_2 at just two excitation wavelengths λ_1 and λ_2 is in principle sufficient to calculate [Ca^{2+}], independent of total dye concentration, path length, or absolute sensitivity of the instrument. Let us assume that dye concentration and path length are small enough for the fluorescence contribution from any given molecular species to be proportional to the concentration of that species. Two wavelengths and two dye species require four proportionality coefficients, hereby symbolized as S_{f1} for free dye measured at wavelength λ_1, S_{f2} for free dye at λ_2, and S_{b1} and S_{b2} for Ca^{2+}-bound dye at λ_1 and λ_2. It is well known that in principle, each S factor is the product of excitation intensity, ln 10, extinction coefficient, path length, quantum efficiency, and the instrumental effi-

---

[4] R. Y. Tsien and M. Poenie, manuscript in preparation.

ciency of collecting emitted photons. In practice, the four S factors are readily measured from the fluorescence intensities of calibration solutions containing known low concentrations of free and Ca²⁺-saturated dye. For a mixture of free and Ca²⁺-bound indicator at respective concentrations, c_f and c_b, the total fluorescence intensities at wavelengths λ_1 and λ_2 will be given by the following.

$$F_1 = S_{f1}c_f + S_{b1}c_b \tag{1a}$$

$$F_2 = S_{f2}c_f + S_{b2}c_b \tag{1b}$$

However, c_f and c_b are related to [Ca²⁺] by the equation for 1:1 complexation,

$$c_b = c_f[Ca^{2+}]/K_d \tag{2}$$

where K_d is the effective dissociation constant. The fluorescence ratio R is the ratio $F_1/F_2 = (S_{f1}c_f + S_{b1}c_b)/(S_{f2}c_f + S_{b2}c_b) =$

$$(S_{f1} + S_{b1}[Ca^{2+}]/K_d)/(S_{f2} + S_{b2}[Ca^{2+}]/K_d) = R \tag{3}$$

Solving for R yields the following calibration equation.

$$[Ca^{2+}] = K_d \left(\frac{R - (S_{f1}/S_{f2})}{(S_{b1}/S_{b2}) - R}\right)\left(\frac{S_{f2}}{S_{b2}}\right) \tag{4}$$

Note that S_{f1}/S_{f2} is simply the limiting value that R can have at zero [Ca²⁺] and so may be considered R_{min}, while S_{b1}/S_{b2} is the analogous limiting R_{max} that the ratio has at saturating [Ca²⁺]. The above equation may therefore be written as:

$$[Ca^{2+}] = K_d \left(\frac{R - R_{min}}{R_{max} - R}\right)\left(\frac{S_{f2}}{S_{b2}}\right) \tag{5}$$

a form closely analogous to the calibration equation for a dye using intensity values at only one wavelength.

$$[Ca^{2+}] = K_d \left(\frac{F - F_{min}}{F_{max} - F}\right) \tag{6}$$

The applicability of both Equations 5 and 6 depends on the assumptions that the dye forms a simple 1:1 complex with Ca²⁺ (Equation 2), that it behaves in cells as it does in calibration media, and that it is sufficiently dilute for fluorescence intensity to be linearly proportional to the concentrations of the fluorescent species (Equation 1). However, Equation 6 requires that F, F_{min}, and F_{max} all be determined at the same instrumental sensitivity, optical path length, and effective total concentration of dye. These requirements are hard to satisfy when observing cells confined to a monolayer or under a microscope or in a flow cytometer, since the only really sure way to measure F_{max} and F_{min} requires lysing the cells and titrating the dye released. Only with disaggregated cells suspended in a cuvette can the dye concentration in the optical path be relied upon to stay unchanged despite lysis. Although methods have been proposed to calibrate without lysis, for example, by using ionophore to saturate the dye with Ca²⁺ then quench it with Mn²⁺ (26), the evidence that ionophore-induced alterations reflect the true end points rests upon comparison to results obtained after cell lysis. Also such methods do not compensate for dye loss due to bleaching or leakage during the main recording period. Using ratios and Equation 5, dye content and instrumental sensitivity are free to change between one ratio and another since they cancel out in each ratio. Of course, stability is required within each individual ratio measurement; also R, R_{min}, and R_{max} should all be measured on the same instrumentation so that any wavelength biases influence all of them equally. The experimental data for fura-2 at excitation $\lambda_1 = 340$ nm and $\lambda_2 = 380$ nm from Fig. 3 correspond well to Equation 5 with $R_{min} =$

0.768, $R_{max} = 35.1$, $S_{f2}/S_{b2} = 15.3$, and $K_d = 135$ nM. Obviously these equations are just as applicable to indo-1 emission ratios. For the data of Fig. 4 at emission $\lambda_1 = 400$ nm and $\lambda_2 = 490$ nm, $R_{min} = 0.121$, $R_{max} = 2.60$, $S_{f2}/S_{b2} = 2.01$, and $K_d = 250$ nM. The term (S_{f2}/S_{b2}) in Equation 5 becomes unnecessary if one chooses λ_2 to be the wavelength at which all the calibration spectra cross one another, so that $S_{f2} = S_{b2}$. Such a choice of λ_2 has been common in previous applications of ratio fluorescence, but we prefer to set λ_1 and λ_2 on opposite sides of the crossover point in order to make full use of the spectral sensitivity of the dye and to increase the range between R_{min} and R_{max}.

Ratio operation has two main disadvantages. If tissue autofluorescence is significant, it has to be subtracted before forming the ratio, whereas it cancels out automatically in Equation 6 as long as it is calcium-independent. Fortunately the greater fluorescence intensity of the new dyes makes autofluorescence less of a problem. The other problem with ratios is that the instrumentation to alternate excitation wavelengths rapidly and to calculate the ratio of fluorescence intensities is not yet commercially available although it ought to be. We have built a system in which two light sources and two monochromators are alternately selected by a butterfly-shaped sector mirror rotating at 10–30 Hz. Cancellation of large fluctuations in intensity has indeed been invaluable in studying monolayers and single small cells. However, it would be relatively difficult to provide sequential excitation wavelengths of stable relative intensity in flow cytometry, so that the emission shift of indo-1 makes it particularly attractive in this application.

The new dyes operate at excitation and emission wavelengths only a little longer than those of quin2, not nearly as far into the visible or infrared as would ultimately be desirable. Nevertheless, fura-2 shows considerable sensitivity to Ca²⁺ at 350 nm and 380–385 nm (Fig. 5), whereas the response of quin2 to Ca²⁺ falls off sharply between 339 and 350 nm. This small difference in acceptable wavelengths is sufficient to make fura-2 much easier to use on conventional fluorescence microscopes with glass optics that typically cut off very abruptly at wavelengths between 340 and 350 nm. Both the wavelengths and Ca²⁺ dissociation constant should increase if groups more strongly electron-withdrawing than carboxylate were to be placed at the far end of the chromophore (compare fura-1 and fura-3). However, such substitution may also decrease quantum yields. Also the terminal carboxylate is at least theoretically attractive as a deterrent of hydrophobic bonding to the long chromophore tail.

The large absorption coefficients of these dyes are just as expected from the length of the chromophore and data on simpler analogs. Although quantum efficiencies cannot be predicted with certainty, extended chromophores with rigid ring structures are well known to be conducive to efficient fluorescence. The hypsochromic shift in absorption and excitation spectra upon binding Ca²⁺ is well understood (6): the Ca²⁺ monopolizes the lone pair of electrons on the amino nitrogen, possibly by twisting the bond between the nitrogen and the ring. The conjugation between the lone pair and the rest of the chromophore is thereby disrupted. Presumably the Ca²⁺ moves away from the nitrogen in the excited state, so that the emission wavelengths differ little between low and high [Ca²⁺]. It is unclear why indo-1 should be an exception.

A marginal advantage of the new indicators over quin2 is their slightly weaker affinities for Ca²⁺. The roughly 2-fold higher dissociation constants for fura-2 and indo-1 compared to quin2 should improve resolution of [Ca²⁺]ᵢ levels above 10⁻⁶ M. A further scale expansion of the upper end of the [Ca²⁺]

scale occurs if fluorescence ratios, for example 340:380 nm excitation for fura-2, are plotted on a linear scale *versus* free $[Ca^{2+}]$. This apparent scale expansion results from the decrease of 380 nm excitation efficiency almost to zero as the dye approaches Ca^{2+} saturation. This mathematical expansion does not actually improve the resolution of high Ca^{2+} values, because static uncertainties and dynamic noise in the individual wavelength traces also get amplified when the denominator approaches zero. If one had chosen to plot 380:340 nm, neither the scale expansion nor noise amplification would occur at high Ca^{2+}. The reason for arbitrarily choosing 340:380 nm over its inverse is that this ratio changes in the same direction as $[Ca^{2+}]$.

A fifth advantage of the new dyes over quin2 is their better selectivity for Ca^{2+} over divalent cations such as Mg^{2+}, Mn^{2+}, Zn^{2+}, and Fe^{2+}. The improvements for fura-2 over quin2 are about 4-fold, 12-fold, and 40-fold for Mg^{2+}, Mn^{2+}, and Zn^{2+}, respectively. Most workers using quin2 have implicitly assumed that cytosolic free Mg^{2+} was 1 mM as was measured in lymphocytes (29) and therefore used in calibration solutions (7). If the true free Mg^{2+} were 0 or 2 mM, respectively, the true $[Ca^{2+}]$ values would be about 0.5 or 1.5 times higher than those estimated assuming 1 mM. The new dyes should be less sensitive yet to uncertainties in Mg^{2+}. The only clear instance of heavy metal interference with quin2 has been in certain tumor cell lines (8), but the reduced heavy metal affinities of the new dyes should help guard against other occurrences as well as toxicity due to chelation of essential heavy metals. These dyes and quin2 might even be used as heavy metal indicators by working at the wavelengths where all the different Ca^{2+} curves cross each other.

The improved divalent cation selectivity of the new dyes is probably due to the abandonment of the quinoline structure with its troublemaking ring nitrogen (6). Magnesium binding affects the spectrum much less than Ca^{2+} binding probably because Mg^{2+} is too small to bind to both amino nitrogens at once (6) and tends to choose the nitrogen on the right side of the structure as drawn, since that one is not in conjugation with the slightly electron-withdrawing chromophoric skeleton. Fura-2 and EGTA both respond to increasing temperature by weakening their Ca^{2+} affinity and increasing their Mg^{2+} affinity (11). This suggests that the thermodynamic bases for their Ca^{2+}/Mg^{2+} selectivities are similar.

At present the preferred dye for most applications would be fura-2, although indo-1 is the prime candidate for flow cytometry. The stilbenes are somewhat easier to synthesize but do not fluoresce as brightly, have complicated problems of photoisomerization and photodecomposition, and are relatively difficult to load as acetoxymethyl esters[5] due to insufficient solubility. It remains to be seen whether the slightly longer wavelengths of fura-3 can compensate for its lower quantum efficiency and less hydrophilic chromophore. The main disadvantages of fura-2 and indo-1 compared to quin2 are logistic: their present commercial unavailability and the need for dual-wavelength instrumentation if one hopes to take full advantage of the wavelength shifts of the new dyes. Some problems in detailed calibration of fura-2 have arisen from an influence of microviscosity on quantum yields, an effect to be discussed in subsequent papers. Nevertheless the new dyes have already made $[Ca^{2+}]_i$ measurements possible in a number of previously intractable systems. The prospect of studying individual cells or aggregated tissue should enor-mously expand the range and ease of optical measurement of $[Ca^{2+}]_i$ and its ubiquitous messenger functions.

REFERENCES

1. Blinks, J. R., Wier, W. G., Hess, P., and Prendergast, F. G. (1982) *Prog. Biophys. Mol. Biol.* **40**, 1–114
2. Tsien, R. Y., and Rink, T. J. (1983) in *Current Methods in Cellular Neurobiology* (Barker, J. L., and McKelvy, J. F., eds) Vol III, pp. 249–312, John Wiley and Sons, New York
3. Campbell, A. K. (1983) *Intracellular Calcium*, John Wiley and Sons, New York
4. Tsien, R. Y. (1983) *Annu. Rev. Biophys. Bioeng.* **12**, 91–116
5. Tsien, R. Y., Pozzan, T., and Rink, T. J. (1984) *Trends Biochem. Sci.* 263–266
6. Tsien, R. Y. (1980) *Biochemistry* **19**, 2396–2404
7. Tsien, R. Y., Pozzan, T., and Rink, T. J. (1982) *J. Cell Biol.* **94**, 325–334
8. Arslan, P., diVirgilio, F., Tsien, R. Y., and Pozzan, T. (1985) *J. Biol. Chem.* **260**, 2719–2727·
9. Lippert, E., Naegele, W., Seibold-Blankenstein, I., Staiger, U., and Voss, W. (1959) *Fresenius' Z. Anal. Chem.* **170**, 1–18
10. Miller, J. N. (ed) (1981) *Standards in Fluorescence Spectrometry*, Chapman and Hall, London
11. Martell, A. E., and Smith, R. M. (1974) *Critical Stability Constants*, Vol. 1, Plenum Press, New York
12. Tsien, R. Y., and Rink, T. J. (1980) *Biochem. Biophys. Acta* **599**, 623–638
13. DiPolo, R., Requena, J., Brinley, F. J., Jr., Mullins, L. J., Scarpa, A., and Tiffert, T. (1976) *J. Gen. Physiol.* **67**, 433–467
14. Owen, J. D. (1976) *Biochem. Biophys. Acta* **451**, 321–325
15. Zucker, R. S., and Steinhardt, R. A. (1979) *Nature (Lond.)* **279**, 820
16. Baker, P. F., and Whitaker, M. J. (1979) *Nature (Lond.)* **279**, 820–821
17. Harafuji, H., and Ogawa, Y. (1980) *J. Biochem. (Tokyo)* **87**, 1305–1312
18. Rossotti, H. (1978) *The Study of Ionic Equilibria*, Longman, London
19. Cadogan, J. I. G. (1979) in *Organophosphorus Reagents in Organic Synthesis* (Cadogan, J. I. G., ed) pp. 269–294, Academic Press, New York
20. Marsh, J. P., Jr., and Goodman, L. (1965) *J. Org. Chem.* **30**, 2491–2494
21. Freifelder, M. (1971) *Practical Catalytic Hydrogenation*, John Wiley and Sons, New York
22. Yamawaki, J., Kawate, T., Ando, T., and Hanafusa, T. (1983) *Bull. Chem. Soc. Jpn.* **56**, 1885–1886
23. Tsien, R. Y. (1981) *Nature (Lond.)* **290**, 527–528
24. Neuenschwander, M., and Iseli, R. (1977) *Helv. Chim. Acta* **60**, 1061–1072
25. Ross, D. L., and Blanc, J. (1971) in *Photochromism* (Brown, G. H., ed) pp. 471–556, John Wiley and Sons, New York
26. Hesketh, T. R., Smith, G. A., Moore, J. P., Taylor, M. V., and Metcalfe, J. C. (1983) *J. Biol. Chem.* **258**, 4876–4882
27. Williams, R. J. P. (1982) *FEBS Lett.* **140**, 3–10
28. Rogers, J., Hesketh, T. R., Smith, G. A., Beaven, M. A., Metcalfe, J. C., Johnson, P., and Garland, P. B. (1983) *FEBS Lett.* **161**, 21–27
29. Rink, T. J., Tsien, R. Y., and Pozzan, T. (1982) *J. Cell Biol.* **95**, 189–196
30. Titley, A. F. (1928) *J. Chem. Soc. (Lond.)* 2571–2583
31. Quackenbush, F. W., Grogan, W. M., Jr., Midland, S. L., Bell, F. P., MacNintch, J. E., Hutsell, T. C., Cruzan, G., and Klauda, H. C. (1977) *Artery* **3**, 553–575
32. *Beilsteins Handbuch der Organisches Chemie* (1967) Drittes Erganzungswerk, Vol. 6, p. 4402, Springer-Verlag, Berlin
33. Schiff, H., and Pellizzari, G. (1883) *Liebigs Ann. Chem.* **221**, 365–379
34. Alonso, M., and Jano, P. (1980) *J. Heterocycl. Chem.* **17**, 721–725
35. Knoevenagel, E. (1913) *Liebigs Ann. Chem.* **402**, 111–148
36. Sayce, I. G. (1968) *Talanta* **15**, 1397–1411

---

[5] R. Y. Tsien and T. Pozzan, unpublished results.

SUPPLEMENTARY MATERIAL to
"A New Generation of Ca²⁺ Indicators with
Greatly Improved Fluorescence Properties"
by Grzegorz Grynkiewicz, Martin Poenie and Roger Y. Tsien

Proton NMR spectra were recorded on Varian instruments at 60 MHz (EM-360), 80 MHz (CFT-20), 90 MHz (EM-390), and 100 MHz (HA-100). Peaks are reported below in the following format: NMR (solvent, operating frequency): chemical shift δ in ppm from tetramethylsilane, multiplicity (s = singlet, d = doublet, dd = doublet of doublets, t = triplet, q = quartet, m = multiplet, br = broad), spin-spin coupling constant if appropriate, integrated number of protons; sometimes several adjacent peaks are too close for their integrals to be separated, in which case only the total integral for a cluster is stated.

I --- > II

57.6 g (0.30 mol) potassium 2-nitro-5-methylphenoxide (I), 187.4 g (1.0 mol) 1,2-dibromoethane, and 151 g dimethylformamide were heated together to 120°. The bright orange colour of the reaction mixture soon faded to pale yellow and a white precipitate was deposited. After cooling, the precipitate was filtered off and washed with water and dichloromethane. The insoluble residue was 1,2-bis(2-nitro-5-methylphenoxy)ethane, 5.87 g (.018 mol). The combined organic phases of the filtrate were washed repeatedly with dilute NaOH until no more orange colour appeared in the extracts, then washed once with saturated aqueous NaCl containing a little NaH₂PO₄. After drying over MgSO₄, the organic phase was evaporated to dryness and the residue recrystallized either from petroleum ether (b.p. 60-80°) or methanol-water. The yield of II was 34 g (44%), m.p. 44-45°. NMR (CDCl₃, 60 MHz) 7.75, d, 8Hz, 1H; 6.9-6.75, m, 2H; 4.36, t, 7Hz, 2H; 3.6, t, 7Hz, 2H; 2.36, s, 3H.

II + III --- > IV

5.32 g (20.5 mmol) II and 3.98 g (22.5 mmol) potassium 2-nitrophenoxide (III) were stirred in 10 ml dimethylformamide and heated to 130° for 80 min. The mixture was cooled, diluted to 100 ml with water, and filtered; the precipitate was washed repeatedly with aqueous Na₂CO₃ and then water. After drying, it was recrystallized from 1250 ml boiling 95% ethanol containing 5 ml acetic acid, to which a little water was added after cooling. The yield of IV was 5.55 g, 85%, m.p. 150-152°. NMR (CDCl₃, 80 MHz): 7.7-6.6, m, 7H; 4.34, s, 4H; 2.26, s, 3H.

IV --- > V

5.55 g IV were hydrogenated at room temperature and atmospheric pressure with .46 g palladium (5% on charcoal) catalyst in 95% ethanol. After full hydrogen uptake (13 hrs), the mixture was warmed, filtered while hot, decolorized with a pinch of NaBH₄, and chilled to -10°; the yield of V as white crystals was 4.03 g, 89%, m.p. 118-119°. NMR (CDCl₃, 80 MHz): 6.8-6.5, m, 7H; 4.28, s, 4H; 3.5-3.7, br s, 4H; 2.24, s, 3H.

V --- > VIa or VIb

2.58 g (10 mmol) V, 11.3 g (53 mmol) 1,8-bis(dimethylamino)naphthalene, .79 g (5.3 mmol) sodium iodide, 8.91 g (53 mmol) ethyl bromoacetate, and 9.5 g acetonitrile were stirred and refluxed under nitrogen for 18 hrs. The cooled mixture was diluted with toluene and filtered. The filtrate was extracted with phosphate buffer at pH2 until the 1,8-bis(dimethylamino)naphthalene was removed. The toluene solution was dried and evaporated and the residue recrystallized from 50 ml ethanol. The yield of the tetraethyl ester, VIa, was 5.27 g, 87%, m.p. 110-110.5°. NMR(CDCl₃, 100 MHz): 6.88-6.6, m, 7H; 4.30, s, 4H; 4.18, s, 4H; 4.14, s, 4.08, q, 7Hz, total 16H; 2,28, s, 3H; 1.18, t, 7Hz, 12H.

In larger-scale repetitions, ethyl bromoacetate was replaced by methyl bromoacetate and 1,8-bis(dimethylamino)naphthalene was replaced by Na₂HPO₄ dried at 150°. Thus 25.83 g (100 mmol) V, 71g (500 mmol) dried Na₂HPO₄, 5.9 g (39 mmol) NaI, 84.7 g (554 mmol) BrCH₂CO₂Me and 104 g CH₃CN were refluxed under nitrogen with vigorous stirring by a crescent-shape paddle for 18 hr. The cooled reaction mixture was partitioned between water and toluene. The organic phase was evaporated to dryness and recrystallized from methanol. The yield of the tetramethyl ester, VIb, was 40.2 g (71%). After another crystallization from methanol, the m.p. was 95-95.5°. NMR (CDCl₃, 90 MHz): 6.83, s, 6.67, m, total 7H; 4.24, s, 4.13, s, 4.09, s, total 12H; 3.56, s, 3.54, s, total 12H; 2.23, s, 3H.

VIb --- > VIIb

2.186g (4.0 mmol) VIb was dissolved with stirring in 4.0 ml of dry dimethylformamide containing 0.4 ml of dry pyridine. The mixture was cooled in an ice bath and phosphorus oxychloride (3.0 ml) was added dropwise. The reaction mixture turned black almost immediately. TLC (pet. ether-ethyl acetate 1:1) showed just a trace of product after 0.5 hr. The reaction mixture was stirred at 60° for 1 hr. and then left covered at room temperature. The reaction mixture was dissolved in 20 ml CH₂Cl₂ and poured onto crushed ice mixed with aqueous NaOH. The aqueous layer was extracted with five 10 ml portions of CH₂Cl₂. The combined organic extracts were dried with MgSO₄, filtered and evaporated. The partially crystalline residue (1.75 g) was triturated with 5 ml isopropyl alcohol, filtered, washed with an ether - pet. ether mixture and dried. Yellowish crystals of VIIb were obtained, homogenous on TLC and melting at 126-7°, weight 1.50 g (65.3%). A second crop of crystals weighed 0.126 g, bringing the combined yield to 72%. Recrystallization from acetone-hexane gave pale yellow crystals, m.p. 131-132°. NMR (CDCl₃, 90 MHz): 9.78, s, 1H; 7.4-7.0, m, 3H; 6.83-6.56, m, 3H; 4.28, s, 4.22, s, 4.10, s, total 12H; 3.58, s, 12H; 2.24, s, 3H.

VIIb + VIII --- > IX

574 mg (1 mmol) VIIb, 4-ethoxycarbonylbenzyltriphenylphosphonium bromide VIII (800 mg, 1.58 mmol), and 0.4 g anhydrous K₂CO₃ were stirred at 100° in 4 ml of dry dimethylformamide for 2.5 hrs. The cooled reaction mixture was partitioned between water and toluene, then the aqueous layer was extracted with more toluene. The residue after evaporating the solvent was chromatographed on silica in petroleum ether - ethyl acetate 9:1(v/v). The mixture of stilbenes was isolated in 0.380 g (53%) yield. Four recrystallizations from ethyl acetate-petroleum ether afforded pure trans-isomer of IX, m.p. 131-132°. The isolation and purification steps were performed under dim orange safelight illumination. NMR (CDCl₃, 90 MHz): 7.79, d, 8Hz, 2H; 7.48, d, 8Hz, 2H; 7.1-6.85, m, 6.8-6.5, m, total 7-8H; 4.4-3.9, m, 14H; 3.58, s, 3.55, s, total 12H; 2.22, s, 3-4H; 1.37, t, 7Hz, 3-5H.

The phosphonium salt (VIII) was prepared in 92% yield by reacting 12.16 g (50 mmol) ethyl p-bromomethylbenzoate, XXVII (30), with 14.48 g (55 mmol) triphenylphosphine in refluxing toluene overnight. The precipitate was filtered off from the cooled reaction mixture. After washing, and drying it had m.p. 241-243°, weighed 23.3 g (92% yield), and was sufficiently pure for further use.

The above phosphonium salt was synthesized with an ethyl rather than a methyl ester group because initial trials were performed with ethyl esters in BAPTA derivatives VI and VII. Later we switched to a large pre-existing stock of slightly less pure VI which happened to have been made with methyl ester groups. The final versions of IX, XII, and XVI reported above were therefore made with four methyl ester groups and one ethyl. Though we observed no sign of scrambling by ester interchange in IX, XII, and XVI, and all ester groups are removed in the final chelators X, XIII, and XVII, it would be more sensible to work with all methyl or ethyl groups if one were starting from scratch.

VII + XI --- > XII

0.486 g (0.84 mmol) VIIb was refluxed overnight with 0.42 g (0.84 mmol) phosphonium salt XI and sodium methoxide (54 mg, 1 mmol) in CH₂Cl₂ overnight. The cooled reaction mixture was partitioned between water and chloroform. The crude product was chromatographed on silica in toluene - ethyl acetate 4:1 (v/v) and isolated as a thick syrup (112 mg, 17% yield). NMR (CDCl₃, 90 MHz): 7.65, d, 9Hz, 2H; 7.4, d, 9Hz, 2H; 7.3-7.0, m, integral obscured by toluene contamination; 6.9-6.5, m, 7H; 4.25, s, 4.20, s, 4.16, s, total 12H; 3.54, s, 12H; 2.77, s, 2.75, s, total 6H; 2.25, s, 3H.

[right column]

Sulfonamide phosphonium salt XI was prepared analogously to VIII by reacting triphenylphosphine with N,N-dimethyl-4-(chloromethyl)benzenesulfonamide in refluxing toluene. Its m.p. was 275-280°. The sulfonamide was prepared by reacting 4-chloromethylbenzenesulfonyl chloride(31) with a cold solution of dimethylamine in ether.

VII + XIV --- > XV

0.14 VIIb, 0.20 g XIV, and 0.6 g K₂CO₃ were stirred 3 hr at 90° in 1 ml dry dimethylformamide. The reaction mixture was partitioned between toluene and water and the organic phase was evaporated and chromatographed on silica with toluene - ethyl acetate 2:1. The product fractions from the column were pooled and evaporated to give a reddish oil weighing 135 mg, 69% yield.

Phosphonium salt XIV (m.p. 165-168) was prepared in 76% yield by reacting 1.5 g triphenylphosphine with 1.2 g ethyl 4-bromomethyl-3-nitrobenzoate in refluxing toluene overnight. The latter ester was prepared by stirring 2.43 g of ethyl p-bromomethylbenzoate, XXVII, in 10 ml concentrated H₂SO₄ at 5°C while adding 1 ml 70% HNO₃ dropwise. The nitration mixture was poured onto crushed ice and extracted with CH₂Cl₂. The extract was washed with dilute NaOH, dried, and evaporated to give an oil, which eventually crystallized, m.p. 41-43°, yield 2.32 g, 80%. NMR (CCl₄, 90MHz): 7.8, d, 9Hz, 7.67, d, 2Hz, 7.58, dd, 9Hz + 2Hz, total 3H; 4.45, s, 2H; 3.9, s, 3-4H.

XV --- > XVI

300 mg (0.392 mmol) XV were dissolved in 2 ml triethyl phosphite and refluxed overnight under nitrogen. The reaction mixture was evaporated to dryness in vacuo, and the residue was chromatographed on silica in toluene-ethyl acetate 4:1. The cyclized product XVI was obtained as a dark oil (160 mg, 56%) which crystallized after drying at 0.1 torr. Recrystallization from methanol produced crystals melting at 96-97°. NMR (CDCl₃, 90 MHz): 9.46, s, 1H; 8.08, s, 1H; 7.73, d, 8Hz, 7.5, d, 8Hz, total 2H; 7.21, m, 2H; 6.9-6.5, m, 5H; 4.35, q, 7Hz, 4.21, s, 4.14, s, 4.09, s, total 12-14H; 3.58, s, 3.54, s, 11-12H; 2.17, s, 3H; 1.8, br s, about 2H (may contain H₂O peak); 1.33, t, 7Hz, 3H.

XVIII --- > XIX

To a stirred suspension of 55 g (0.5 mol) hydroquinone (XVIII) and 143.1 g (1.1 mol) benzyl chloride in 100 ml ethanol was added a solution of 60.2 g (0.91 mol) potassium hydroxide in ethanol. After 1 hr the mixture was poured into water. The precipitate was filtered off several hours later, dried at 70°, and recrystallized from 3.5 liters of boiling ethanol. The yield of XIX was 105 g, 73%, m.p. 128-130° (literature values(32) range from 126.5 to 130°). NMR (CDCl₃, 100 MHz): 7.35, s, 10H; 6.87, s, 4H; 4.98, s, 4H.

XIX --- > XX

18.3 g (.203 mol) 70% aqueous nitric acid were diluted to 50 ᴍ with glacial acetic acid and added to a suspension of 58 g (.200 mol) XIX in 200 ml acetic acid. The mixture was stirred and gently warmed to 50°, whereupon the starting material dissolved and product began to crystallize out. After cooling the mixture and filtering off a first crop, water was added dropwise to precipitate a second crop. The total yield of XX was 65.6 g, 98%, m.p. 81-82.5° (83° was reported in ref. 33). NMR (CDCl₃, 100 MHz): 7.5-6.9, m, 13H; 5.15, s, 5.03, s, total 4H.

XX --- > XXI

A solution of 50.4 g (.15 mol) XX in 100 ml ethanol-free chloroform was treated with 15.0 ml (0.2 mol) trifluoroacetic acid and kept at room temperature for 48 hours, at which time an NMR spectrum showed ca. 90% conversion of the starting material, as judged by the reduction of the peak near δ = 5.08, the lower-field member of the pair of benzylic CH₂ resonances. The excess acid was neutralized with 5M aqueous potassium hydroxide. The organic phase was repeatedly extracted with dilute aqueous potassium carbonate until the aqueous layer was pale orange instead of dark brown as at first. The chloroform solution was then diluted with 1.5 volumes of diethyl ether and treated with 60 ml 5M potassium hydroxide. The dark red precipitate of potassium 4-benzyloxy-2-nitrophenoxide was filtered off, acidified with dilute HCl, and extracted with six 600 ml portions of petroleum ether. After combining the extracts and evaporating the petroleum ether, the residue was recrystallized from boiling methanol to which water was added dropwise after cooling. The yield of XXI was 31-32 g, 84-87%, m.p. 67-70°. NMR (CCl₄, 100 MHz): 10.24, s, 1H; 7.52, d, 3Hz, 1H; 7.32, s, 5H; 7.19, dd, 3Hz and 9Hz, 7.00, d, 9 Hz, 1H; 5.01, s, 2H.

XXI + II --- > XXII

A mixture of 2.45 g (10 mmol) XXI, 2.8 g (10.8 mmol) II, 0.76g (5.5 mmol) anhydrous K₂CO₃, and 5 ml dimethylformamide was heated to 140° and stirred for 15 min. While still fairly warm, the stirred mixture was treated dropwise with water until the initial deposit of KBr dissolved and the product began to crystallize. It was filtered off, dried (crude yield 90%), and recrystallized by dissolving in a minimum quantity of hot acetone and precipitating with twice its volume of petroleum ether. The light yellow crystals of XXII had m.p. 143-144°. NMR (CDCl₃ + CD₃SOCD₃, 90 MHz): 7.72, d, 9Hz, 1H; 7.5-7.0, m, 8H; 6.87, d, 9Hz, 1H; 5.11, s, 1.5-2H; 4.47, s, 4H; 2.39, s, 3H.

XXII --- > XXIII

5 g (11.8 mmol) XXII and 0.5 g of 5% platinum on charcoal were suspended in 100 ml absolute ethanol and stirred under hydrogen at atmospheric pressure. The theoretical volume was taken up in 5 hrs. but the mixture was left under hydrogen overnight, after which the cumulative uptake was 19% higher than theoretical. Another 5 g of XXII added to the same hydrogenation mixture also took up the same higher-than-theoretical amount of hydrogen overnight. The product XXIII was recrystallized from acetone and had melting point 129-132°. The NMR spectrum showed that the benzyl groups had not been lost. (CDCl₃ + CD₃SOCD₃, 90 MHz): 7.29, s, 5H; 6.75-6.45, m, 4H; 6.32, d, 3Hz, 1H; 6.12, dd, 3Hz + 7Hz, 1H; 4.93, s, 2H; 4.3, br s, 4.22, s, total 8H; 2.18, s, 3H.

XXIII --- > XXIV

3.64 g (10 mmol) XXIII, 10.72 g (50 mmol) 1,8-bis(dimethylamino)naphthalene, 2.0 g (13 mmol) dried NaI, 33.5 g (50 mmol) ethyl bromoacetate, and 15 ml acetonitrile were stirred and refluxed under nitrogen for 40 hrs, with a further addition of 1.5 ml ethyl bromoacetate and 2 g 1,8-bis(dimethylamino)naphthalene after the first 24 hrs. The cooled reaction mixture was evaporated to dryness, diluted with toluene and filtered; the gray precipitate was washed repeatedly with further small portions of toluene. The pooled toluene solutions were repeatedly extracted with phosphate buffer until the washings had the same pH, 2, as the fresh buffer. The toluene solution was then washed with water and dried over MgSO₄. After evaporation of the toluene under reduced pressure, the residue was washed with petroleum ether-ethyl acetate 9:1 v/v to remove traces of ethyl bromoacetate. The yield of XXIV was 6.4 g (90%), m.p. 95-96°. NMR (CDCl₃, 90 MHz): 7.33, s, 5H; 6.86-6.36, m, 5-6H; 4.96, s, 2H; 4.20, s, 4.12, s, 4.10, s, 4.03, q, 7Hz, total 20H; 2.23, s, 3H; 1.15, t, 7Hz, 12H.

XXIV --- > XXV

0.35 g (0.5 mmol) XXIV was dissolved in 2 ml of dry dimethylformamide and 0.4 ml pyridine. POCl₃ (0.4 ml, 4 mmol) was added slowly with stirring at 0°. After 0.5 hr, the black reaction mixture was allowed to warm up and was left overnight at room temperature. The reaction mixture was neutralized with ice-cold aqueous NaOH and extracted with three 20 ml portions of toluene. Evaporation of the toluene phases gave crystalline XXV, m.p. 114-115° (256 mg, 73% yield). NMR (CDCl₃, 90 MHz): 10.33, s, 1H; 7.35, s, 5-7H; 6.8-6.6, m, 4H; 6.3, s, 1H; 5.08, s, 2H; 4.25-3.9, m, 20H; 2.21, s, 3-4H; 1.14, t, 7Hz, 12-14H.

XXV --- > XXVI

XXV was debenzylated by hydrogenation in glacial acetic acid with 5% Pd on charcoal as catalyst. The substrate concentration was 0.1 M. At room temperature and 1 atm H₂, the reaction proved complete after overnight

stirring. The mixture was filtered, the catalyst washed with ethyl acetate, the filtrate evaporated at reduced pressure, and the residue crystallized from acetone-hexane. XXVI had m.p. 109-111°. NMR (CDCl₃, 90MHz): 11.1, br s, 1H; 9.59, s, 1H; 6.93, s, 1H; 6.74-6.60, m, 3H; 6.14, s, 1H; 4.22, s, 4.11, s, 4.10, q, 7Hz, total 20H; 2.24, s, 3H; 1.17, t, 7Hz, 12H.

XXVI + XXVII --->XXVIII

Although a low yield of impure XXVIII can be obtained directly by heating XXVI and XXVII in DMF at 100°for 70 hr, it is better to do the esterification and furan ring closure in separate steps. 65 mg XXVI (0.1 mmol), 50 mg ethyl 4-bromomethylbenzoate (XXVII), 0.2 g K₂CO₃, and 10 mg tetrabutyl-ammonium hydrogen sulfate were stirred overnight under reflux in acetonitrile. The product, the 4-ethoxycarbonylbenzyl ether of XXVI was isolated by preparative layer chromatography with petroleum ether-ethyl acetate 1:1, giving 57 mg, 71% yield, m.p. 109-110°. NMR (CDCl₃, 90 MHz): 10.34, s, 1H; 8.06, d, 8Hz, 2H; 7.47, d, 8Hz, 2H; 7.3, s, partly obscured by CHCl₃; m, 6.8-6.55, 3H; 6.3, s, 1H; 5.16, s, 2H; 4.37, q, 7Hz, 4.21, s, 4.14, s, 4.05, q, 7Hz, 4.02, q, 7Hz, total 22 H; 2.23, s, 3H; 1.38, t, 7Hz, 1.17, t, 7Hz, 1.15, t, 7Hz, total 15H. 39 mg of this ether (.05 mmole) was stirred with potassium fluoride/alumina reagent(22) in 1 ml dimethylformamide for 2 hrs at 150°. The fluorescent product was isolated in 21 mg (54%) yield by preparative layer chromatography on silica with toluene-ethyl acetate 1:1. Longer reaction times in DMF lead to increasing water hydrolysis. NMR (CDCl₃, 90 MHz): 8.15, d, 9Hz, 7.89, d, 9Hz, total 4-5H; 7.15-7.05, m, 6.78, m, total 6-7H; m, 3.9-4.5, 20-22H; 2.23, s, 3H; 1.0-1.4, m, 13-17H.

XXVI + XXX ---> XXXI

In this case, ether formation and furan ring closure can be done in one step. 0.5 g (0.77 mmol) XXVI, 0.2 g ethyl 2-chloromethyloxazole-5-carboxylate (XXX), and 0.5 g K₂CO₃ were stirred in 2 ml dry dimethylformamide at 100° for 1.5 hr. The reaction mixture was cooled, diluted with water, acidified with HCl and extracted with CHCl₃. The combined extracts were dried with MgSO₄ and evaporated to a dark, semicrystalline residue. Filtration through a short column of silica gel washed with 1:1 toluene-ethyl acetate gave after evaporation yellow crystals, which after trituration with hexane-ethyl acetate 9:1 and filtration melted sharply at 138°. The yield was 420 mg, 68%. NMR (CDCl₃, 90 MHz): 8.11, s, 1H; 7.69, s, 1H; 7.34, s, 7.29, s, total 2H; 6.97 - 6.87, m, 3H; 4.57, q, 7Hz, 4.45, s, 4.35, s, 4.25, s, 4.22, q, 7 Hz, 4.18, q, 7 Hz, total 22 H; 2.31, s, 3H; 1.44, t, 7 Hz, 3H; 1.21, t, 7Hz, 1.19, t, 7Hz, total 12H.

Ethyl 2-chloromethyloxazole-5-carboxylate (XXX) was prepared by reacting chloroacetonitrile with ethyl diazopyruvate in analogy to the synthesis (34) of ethyl 2-methyloxazole-5-carboxylate. Ethyl diazopyruvate, 0.1g, a few mg of cupric acetylacetonate, and 0.4 ml of chloroacetonitrile were kept overnight at 60° in benzene solution. The cooled reaction mixture was partitioned between aqueous NaHCO₃ and ether. The organic layer was dried, evaporated, and chromatographed on silica, eluting with petroleum ether-ethyl acetate 9:1 v/v. The product isolated was further purified by bulb-to-bulb distillation at 12 torr, 90° air bath temperature. Though the NMR spectrum still showed significant impurities, GC-MS analysis showed that by far the dominant fraction had the correct parent M/e = 189 and isotopic pattern expected for XXX, with fragments at 161 (-C₂H₄ or -CO), 154 (-Cl), 144 (-OC₂H₅), and a base peak at 116 (-COOC₂H₅).

XXVI + XXXIII--->XXXIV

140 mg (0.22 mmol) XXVI, 88 mg (0.58 mmol) p-cyanobenzyl chloride (XXXIII), 350 mg K₂CO₃, and 30 mg tetrabutylammonium hydrogen sulfate were stirred in 3 ml dimethylformamide for 4 hrs at 125°. The dark reaction mixture was diluted with water and extracted into toluene. The evaporated toluene phase was chromatographed on silica with a toluene-ethyl acetate mixture. A fast-running fluorescent band was discarded; the subsequent main peak was evaporated to give 82 mg oil, which crystallized. Further recrystallization from petroleum ether-ethyl acetate gave m m.p. of 120-121°, though a better solvent could probably be found. The yield was 51%. The NMR was crudely as expected, but not precisely assignable. NMR (CDCl₃, 90 MHz): 7.9-7.1, m, 7.03, m, 6.70, m, 4.1-4.3, m, 2.25, s, 0.8-1.4, m.

Saponification and re-esterification with acetoxymethyl groups

Ethyl or methyl esters were saponified to free chelator polyanions by dissolving the ester in a water-miscible solvent such as methanol, ethanol, or dioxane and adding excess aqueous sodium, potassium, or tetrabutylammonium hydroxide. Sometimes brief warming was helpful to start the hydrolysis of esters that precipitate upon addition of aqueous solutions. As long as the chelator had been in homogeneous solution containing at least 0.1M excess NaOH or KOH for a few hours, hydrolysis was complete as judged by thin layer chromatography on silica with butanol-acetic acid-water 4:1:1 or 4:1:5 v/v, or by Ca²⁺ titration. Tetrabutylammonium hydroxide seemed to be slower, perhaps because the cation was less able than K⁺ or Na⁺ to pair with and partially neutralize the charge of intermediate stages of hydrolysis, so that electrostatic repulsion of hydroxide slowed further hydrolysis.

Acetoxymethyl bromide, CH₃COOCH₂Br, was prepared by stirring 4.0 g (30 mmol) methylene diacetate and 5.0 g (33 mmol) trimethylsilyl bromide, in the presence of 60 mg anhydrous ZnCl₂ but no added solvent, for 48 hr at room temperature. The product was distilled crudely at 10 torr, 40-60°, then refractionated through a Vigreaux column at 10 torr, 55-57°, yielding 4.04 g, 87%, containing no detectable BrCH₂OCH₂Br by NMR. Lewis acid catalysis is essential; without it there is no reaction even at 110° in a sealed tube overnight. Methylene diacetate was prepared from paraformaldehyde and acetic anhydride(35) and was carefully distilled to remove CH₃COOCH₂OCH₂OCOCH₃.

Determination of metal ion binding constants

Calcium and magnesium affinities of EGTA at higher ionic strength were measured by titrating 125 µmole portions of EGTA (Fluka Chemical, puriss grade) with 1.00 M KOH (J.T. Baker, low in carbonate). The EGTA was dissolved in 25 ml medium containing 225 mM KCl, 25 mM NaCl, and in some runs 10 mM CaCl₂ or 21 mM MgCl₂. This solution was stirred in a Radiometer TTA80 Titrator, bubbled continuously with nitrogen, and thermostated at 18°C while KOH was added in .005 or .01 ml aliquots from a ABU80 autoburet. The pH was measured with a PHM84 meter, a G2040C electrode and an Ag/AgCl reference electrode connected to the titration solution by a long length of .01" catheter tubing filled with 3M KCl; this electrode chain was calibrated with phthalate (4.001), phosphate (6.889), and borax (9.245) buffers made according to National Bureau of Standards recipes. The fifty to eighty pH readings in each titration were analyzed by the FORTRAN program SCOGS of Sayce (36). The resulting proton ionization constants for EGTA were 9.537 and 8.961 with computed uncertainties of ± .012 and ± .008 respectively. These pK_a values are "mixed" constants, i.e. a_{H+}[EGTA⁴⁻]/[H·EGTA³⁻] = 10⁻⁹·⁵⁴ M where a_{H+} = 10⁻ᵖᴴ. The log absolute stability constants for Ca·EGTA and Mg·EGTA were calculated to be 10.777 ± .011 and 4.567 ± .021; the proton pK_a's for Ca·EGTA and Mg·EGTA came out at 3.51 ± .49 and 7.885 ± .05 respectively. At this ionic strength and any pH > 4, the effective stability constant K'_{Ca} may be calculated as (antilog 10.77)·[1 + antilog (3.51 - pH)]/ [1 + antilog (9.537 - pH) + antilog (9.537 + 8.961 - 2 · pH)] in units of liters/mole. Analogously K'_{Mg} = (antilog 4.567)·[1 + antilog (7.885 - pH)]/ [1 + antilog (9.537 - pH) + antilog (9.537 + 8.961 - 2 · pH)]

Affinities of stil-1 and fura-2 for Zn²⁺ were measured by titrating 1-2 µM dye in 120 mM KCl, 5 mM K₂H₂EGTA, 10 mM MOPS, 5 mM Tris, with 1 M ZnCl₂ dispensed from a micrometer syringe. At each stage of the titration (13 steps from 0 to 7 mM total ZnCl₂ added) the pH was adjusted with base to be within .02 units of 7.12, the actual pH values was noted for computation of pZn, and the excitation spectrum was recorded at room temperature. The family of spectra had a roughly similar appearance to Fig. 3 and was likewise analyzed by Hill plots of the fluorescence at 340 and 380 nm, i.e., by plotting log [(F - F_{min})/(F_{max} - F)] vs. log [free Zn²⁺] where F_{min} and F_{max} are the fluorescences at zero and excess Zn²⁺ respectively. For computation of free Zn²⁺, the effective dissociation constant of EGTA for Zn²⁺ was taken to be 4.27 nM at pH 7.11 and to decrease by .02 log unit per .01 increase in pH (11).

Since Mn²⁺ and Fe²⁺ quench fura-2, the affinities for these ions relative to Ca²⁺ could be assessed by direct competition between the metal ions each in stoichiometric excess. This method, similar to that of Hesketh et al(26), does not involve EGTA or other buffers. Fluorescences of 0.5 µM fura-2 at room temperature were recorded in solutions containing 100 mM KCl, 10 mM KMOPS, pH 7.2. One series also contained 0, 0.1, or 1 mM MnSO₄ and 0, 1.1, 2.2., 4.4, or 8.8 mM CaCl₂; another series had 2 mM CaCl₂ and 0, 0.1, 0.2, 0.5, 1, 2 mM Fe(NH₄)₂(SO₄)₂; and a third series with 0.2 mM Fe(NH₄)₂(SO₄)₂ and 0, 0.2, 0.4, 0.8, 2, 4, and 8 mM CaCl₂. Measurements with Fe(II) were made in a cuvet sealed by a septum and continually bubbled with nitrogen; the solutions stayed clear and nearly colorless until the septum was removed after the end of the experiment, whereupon deposition of yellow Fe(OH)₃ followed rapidly.